Available online at www.sciencedirect.com
SCIENCE DIRECT®
Wave Motion 40 (2004) 399–412
WAVE MOTION
www.elsevier.com/locate/wavemoti

Green's-function method for modeling surface acoustic wave dispersion in anisotropic material systems and determination of material parameters☆

V.K. Tewary*

National Institute of Standards and Technology, Boulder, CO 80305, USA

Received 26 November 2003; received in revised form 27 January 2004; accepted 5 February 2004

Available online 28 July 2004

Abstract

A Green's-function method for modeling propagation of surface acoustic waves in anisotropic nanolayered materials is reviewed. The mathematical model, developed at NIST, provides a computationally efficient inversion algorithm for determination of the material parameters of the film, such as its elastic constants and density, from observed dispersion of the surface acoustic waves. The application of the method to a 306 nm thick TiN film having transverse isotropy on a single crystal Si substrate is discussed as an example. The errors in the values of the parameters determined by using the inversion algorithm and the question of uniqueness of the values of the parameters are discussed in detail. It is suggested that, at least in the example considered in this paper, the SAW dispersion can be used to determine any two parameters of the film, provided other parameters are known by independent measurements. In particular, the values of c_{11} and the density of the film, obtained from the measured SAW dispersion, are the most reliable and the value of c_{44} is the least reliable. The method is extended to account for defective bonding between the film and the interface and the effect of an intermediate layer of silica between the film and the substrate.

Keywords: Elastodynamic Green's function; Materials' characterization; Silicon; Surface acoustic waves; Titanium nitride

1. Introduction

With the advent of nanotechnology, there is a strong current interest in the study of propagation of surface acoustic waves (SAWs) in anisotropic thin films on anisotropic solids for the purpose of elastic characterization of thin films. In a homogeneous semi-infinite solid, the velocity of the surface wave or the Rayleigh wave is independent of the frequency of the wave. For a film of finite thickness on a substrate, the SAW velocity depends upon the frequency. The characteristic features of SAW in thin films arise because of the finite thickness of the film and the coupling between the waves in the film and the substrate. The functional dependence of the phase velocity on the frequency is called the dispersion relation. If the phase velocity is dispersive, so would be the group

☆ Contribution of the National Institute of Standards and Technology, an agency of the US Government. Not subject to copyright.

* Tel.: +3034975753; fax: +3034975030.
E-mail address: tewary@boulder.nist.gov (V.K. Tewary).

0165-2125/$ – see front matter © 2004 Elsevier B.V. All rights reserved.
doi:10.1016/j.wavemoti.2004.02.007

velocity. Usually, however, SAW dispersion relations refer to the variation of the phase velocity. In this paper, therefore, by "velocity" we mean only the phase velocity. The measured SAW dispersion curves have been used [1,2] for estimating the elastic constants of the film and other material parameters such as the density and the thickness.

A mathematical model is needed for interpretation and inversion of SAW dispersion curves to obtain the material parameters of the solid. In this article, we review and discuss a model [3] developed at NIST that is based upon the use of the delta-function representation of the elastodynamic Green's function for anisotropic solids [4]. The SAW dispersion relations are obtained from the poles of the Green's function without any need for numerical integration. This model is computationally efficient and leads to a useful algorithm for inversion of SAW dispersion curves to obtain the material parameters of thin films. We discuss the limits of the inversion algorithm and errors in the determination of the parameters which were not discussed in [3]. We also extend the model given in [3] to two and more layers on the substrate and include the effect of defective bonding between a film and the substrate.

No attempt is made in this article to give an exhaustive review of the published work on SAW dispersion. Extensive literature is already available on various properties of SAWs. See, for example, [5,6] and other references quoted in those papers. Various representations of the elastodynamic Green's function are available in the literature [7–9]. Ting [10] has discussed elastic anisotropy in considerable detail and described some useful models in a recent treatise.

In general, elastic wave propagation provides a useful technique for characterization of materials (see, for example, [11,12], which also give other references). Several features of surface- and guided-wave propagation in anisotropic solids have been discussed in [13–17]. Computational methods for inversion, that is, determination of elastic constants by using the measured wave propagation characteristics in homogeneous anisotropic solids have been described in [18,19], which also give other references. In most of the methods of inversion, one calculates the velocity of the elastic waves as function of the frequency and obtains the material parameters of the film by a least squares fitting between the calculated and the observed dispersion curve. The inversion algorithm [3] developed at NIST provides a direct method that is computationally more efficient and suitable for anisotropic material systems such as layered single crystals which are used in technological applications. In the NIST method the observed dispersion relations for SAW are substituted in the expressions for the poles of the Green's function which results in a set of nonlinear equations for the material parameters of the film.

As an example and a model case, we discuss the dispersion of SAWs in a polycrystalline textured TiN film on single-crystal Si. Currently there is a strong interest in TiN coatings on Si because of the hardness properties of TiN. However, our interest in this paper is not in determining the parameters of a specific TiN film. We simply use this as a model case for discussing the reliability of the parameters predicted by the inversion algorithm. We also calculate the effect of an intermediate layer of fused silica between the film and the substrate on the SAW dispersion curves. Finally, we extend the model to account for a defective interface between the film and the substrate.

The Green's-function method is especially useful to calculate the displacement field or the wave forms, which, in principle, can provide additional information about the material parameters of the film. However, a direct comparison between theoretical and experimental waveforms is difficult because the waveforms depend upon the space–time behavior of the applied force, which is difficult to quantify experimentally. On the other hand, the wave velocities depend only upon the material properties of the solid. Our interest in this paper is in the calculation of SAW dispersion curves and estimating the material parameters of the film by comparing the theoretical and experimental values of SAW velocities. We will therefore not discuss the calculation of the displacement field.

Section 2 gives a review of the Green's-function method for calculating SAW velocities in layered structures. This section also gives an extension of the earlier formulation [3] to incorporate the effect of defective interfacial bonding and an intermediate layer on the SAW dispersion. The inversion algorithm for determination of the material parameters of the film from measured SAW dispersion curves and a detailed discussion of the limitations of the method and associated errors are given in Section 3. The discussion is based upon the case of a 306 nm TiN film on single crystal Si that has been chosen as an example. Finally, conclusions are given in Section 4.

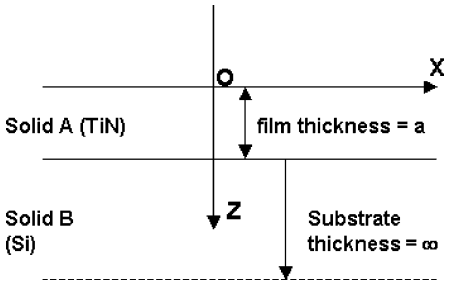

Fig. 1. Cartesian frame of reference for modeling SAW propagation in thin films on a substrate. The point O on the surface is the origin of the coordinates. The *Y*-axis is normal to the plane of the paper.

2. Propagation of SAW in thin films on anisotropic substrates

We consider an anisotropic thin film on an anisotropic substrate. The film and the substrate are indicated as solids A and B, respectively, in Fig. 1 that also shows the Cartesian frame of reference. The solid B extends to infinity in the +Z-direction. Both A and B extend to infinity in the *XY*-plane. We denote the space variables by position vectors $\mathbf{x}$ and $\mathbf{x}'$. Their Cartesian components are denoted by indices 1, 2, and 3, corresponding to *X*, *Y*, and *Z* coordinates, respectively. We denote the time variable by t and its canonically conjugate variable by ω. For positive values, ω can be identified as the angular frequency. Summation over repeated indices is implied.

We calculate the response of the composite solid to a point force applied at the free surface of solid A at $\mathbf{x} = 0$. We assume that there are no body forces in solids A or B. We seek the solution of the homogeneous Christoffel equation:

$$L_{ij}u_j(\mathbf{x}, t) = 0 \tag{2.1}$$

where u is the displacement field,

$$L_{ij} = c_{ikjl}\frac{\partial^2}{\partial x_k \partial x_1} - \rho\frac{\partial^2}{\partial t^2} \tag{2.2}$$

the indices i, j, k, and l assume the values 1, 2, or 3; ρ is the density of the solid; and $\boldsymbol{c}$ is the fourth-rank elastic-constant tensor. We obtain the solution of Eq. (2.1) separately for solids A and B and apply appropriate boundary and continuity conditions at the interface between A and B and the free surface of the solid A. The elastic constant tensor and the density of solids A and B will be identified by adding superscripts A and B, respectively. We will write the solution of Eq. (2.1) in the slowness space [4,14] defined by the slowness vector $\mathbf{q}$ that has the dimensions of inverse velocity.

For notational convenience we introduce a 2D vector $\boldsymbol{\chi}$ in the vector subspace of $\mathbf{x}$ such that $\mathbf{x}$ can be written as $(\boldsymbol{\chi}, x_3)$. Obviously $\chi_1 = x_1$, $\chi_2 = x_2$. Similarly, we define a 2D vector $\boldsymbol{\xi} = (\xi_1, \xi_2)$ in the vector subspace of $\mathbf{q}$ such that $\xi_1 = q_1$ and $\xi_2 = q_2$ and $\mathbf{q} = (\boldsymbol{\xi}, q_3)$. The traction vector $\mathbf{T}$ in the *Z*-direction, with superscripts A or B, is defined as follows:

$$T_i(\mathbf{x}, t) = \tau_{i_3}(\mathbf{x}, t) \tag{2.3}$$

where τ is the stress tensor given by

$$\tau_{im}(\mathbf{x}, t) = c_{imjk}\frac{\partial u_j(\mathbf{x}, t)}{\partial x_k} \tag{2.4}$$

We specify boundary conditions (i) and (ii) for $(-\infty < t < \infty)$ as given below:

i. At $x_3 = 0$ (the top surface), $\mathbf{x} = (\boldsymbol{\chi}, 0)$

$$T^{\mathrm{A}}{}_i(\boldsymbol{\chi},\ x_3 = 0,\ t) = \eta_i \delta(\chi) \exp(\iota\omega t) \tag{2.5}$$

The 3D vector $\boldsymbol{\eta}$ denotes the strength of the load applied at the origin and δ denotes the Dirac delta function. We have assumed the time dependence of the applied load in Eq. (2.5) to be harmonic because our objective is to calculate the dispersion of SAW. The propagation of a $\delta(t)$ pulse has been discussed in [3,20–22].

ii. At $x_3 = a$ (the interface), $\mathbf{x} = (\boldsymbol{\chi}, a)$

$$T^{\mathrm{A}}{}_i(\chi, x_3 = a, t) = T^{\mathrm{B}}{}_i(\boldsymbol{\chi}, x_3 = a, t) \tag{2.6}$$

$$u^{\mathrm{A}}{}_i(\boldsymbol{\chi}, x_3 = a, t) = \boldsymbol{\beta} u^{\mathrm{B}}{}_i(\boldsymbol{\chi}, x_3 = a, t) \tag{2.7}$$

where $\boldsymbol{\beta}$ is a diagonal matrix with components:

$$\beta_{ij} = \beta_i \boldsymbol{\delta}_{ij} \tag{2.8}$$

Eq. (2.5) specifies a free surface except at the origin where the load is applied, and Eq. (2.6) is the continuity condition for the traction at the interface. For a perfectly bonded interface $\boldsymbol{\beta} = \mathbf{I}$ where $\mathbf{I}$ is the unit matrix. The case of perfectly bonded interface has been discussed in detail in [3]. Boundary conditions for a liquid coupled layer have been given by Ren et al. [22]. Non-unity values of β represent a defective interface showing discontinuity of displacement or debonding at the interface. We will refer to β as the debonding parameter. Note that even for a defective interface the traction should be continuous or otherwise there will be a net force at the interface. In addition to the conditions given by Eqs. (2.5) and (2.8), we require $\tau^{\mathrm{B}}{}_{i3}(\mathbf{x}) \to 0$ as $x_3 \to \infty$.

Now we write the solution of Eq. (2.1) using the delta-function representation of the Green's function [3]. Since we need to satisfy three boundary conditions, we introduce three different virtual forces $\mathbf{f}_0$, $\mathbf{f}_\mathrm{a}$, and $\mathbf{f}_\mathrm{b}$ and write the solution in solid A as follows:

$$\mathbf{u}^{\mathrm{A}}(\mathbf{x}, t) = \int \mathbf{G}^{\mathrm{A}}{}_h(\mathbf{q}) \delta[\mathbf{q}\cdot\mathbf{x} - (t - t')] f_0(\boldsymbol{\xi}, t')\, \mathrm{d}\mathbf{q}\, \mathrm{d}t' + \int \mathbf{G}^{\mathrm{A}}{}_h(q^*) \delta[\mathbf{q} * \mathbf{x} + q_3 a - (t - t')] f_a(\boldsymbol{\xi}, t')\, \mathrm{d}\mathbf{q}\, \mathrm{d}t' \tag{2.9}$$

where

$$\mathbf{G}_\mathrm{h}(\mathbf{q}) = \mathrm{M}(\mathbf{q}) \delta(\mathrm{D}(\mathbf{q})) \tag{2.10}$$

$D(\mathbf{q})$ is the determinant of the matrix $[\Lambda(\mathbf{q}) - \rho\mathbf{I}]$, and $\mathbf{M}(\mathbf{q})$ is the matrix of its cofactors, $\mathbf{q} = (q_1, q_2, q_3)$, $\mathbf{q}^* = (q_1, q_2, -q_3)$, $\mathrm{d}\mathbf{q} = \mathrm{d}q_1 \mathrm{d}q_2 \mathrm{d}q_3$, and

$$\boldsymbol{\Lambda}_{ij}(\mathbf{q}) = c_{ikjl} q_k q'_l \tag{2.11}$$

The solution in solid B is written as:

$$\mathbf{u}^{\mathrm{B}}(\mathbf{x}, t) = \int \mathbf{G}^{\mathrm{B}}{}_h(\mathbf{q}) \delta[\mathbf{q}\cdot\mathbf{x} - q_3 a - (t - t')] \mathbf{f}_a(\xi, t')\, \mathrm{d}\mathbf{q}\, \mathrm{d}t' \tag{2.12}$$

In view of the boundary conditions given by Eqs. (2.5)–(2.7), the virtual forces will be independent of q_3. The integrations in Eqs. (2.9) and (2.12) are to be performed over the entire space of $\boldsymbol{q}$ and t'. For brevity the integration limits and separate integration symbols for the variables are not written in Eqs. (2.9) and (2.12). The virtual forces are calculated by a straightforward application [3] of Eqs. (2.5), (2.7), (2.9) and (2.12) which give the harmonic wave forms in solids A and B. The Green's function is given by the displacement field for unit η.

It is found that the Green's function has poles at certain values of ω. The location of the poles are given by the solution of the equation:

$$D_\mathrm{V}(\boldsymbol{\xi}, \omega, c_{ij}, \rho, a) = 0 \tag{2.13}$$

where D_V is the determinant of the set of algebraic equations which determine the virtual forces. It depends upon the material parameters of the film and the substrate such as the elastic constants, density, and the thickness.

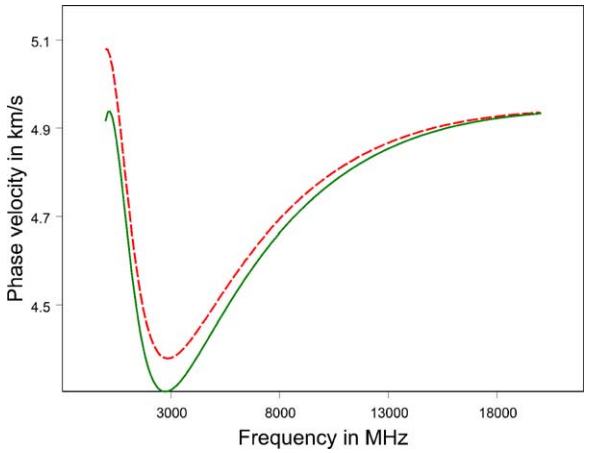

Fig. 2. Dispersion curves in the [1 1 0] and [1 0 0] directions for a perfectly bonded 306 nm TiN film on Si calculated by using material parameters of the reference set in Table 1. Thickness of the film is 306 nm. Solid line: [1 1 0]; dashed line: [1 0 0].

Eq. (2.13) is a nonlinear $3n \times 3n$ determinantal equation where n is the dimensionality of the solid. For 3D, $n = 3$ and for 2D, $n = 2$. The full expression for D_V is given in Ref. [3]. The relationship between the velocity and the frequency obtained by solving Eq. (2.13) gives the dispersion of the SAW. In principle, the elastic constants and other material parameters of the film can be determined by comparing the calculated and measured dispersion of surface waves.

The above formalism is easily extended to incorporate the effect of an intermediate layer between the film and the substrate. We label the intermediate layer as C. The boundary condition at the top surface (solid A) remains the same as given by Eq. (2.5). The continuity conditions at the interface between A and C and between C and B are given by equations exactly similar to Eqs. (2.6) and (2.7). Since there are five conditions to be satisfied, we need to introduce five virtual forces. The determinant D_V will now be $5n \times 5n$ where, as before, $n = 3$ for a 3D problem (point source) and $n = 2$ for a 2D problem (line source). The SAW velocities are obtained by solving the determinantal equation similar to Eq. (2.13) which will now be $5n \times 5n$.

As an example we calculate the dispersion curves for a 306 nm TiN film on a single crystal Si. We chose this example because of a strong current interest in TiN films due to their attractive hardness properties and because good measurements [1,2] and a preliminary analysis [3] of SAW dispersion are available for TiN on Si. The film studied in the measurements was polycrystalline with preferred orientation (texture) in its own crystallographic [1 1 1] direction. The TiN single crystal has fcc structure and therefore has hexagonal symmetry in a plane normal to the [1 1 1] direction. Since the crystallites are randomly oriented on this plane, the film can be assumed to be transversely isotropic.

In our calculations we assume the same geometry as in the experimental set up [1,2] and in Ref. [3]. The measurements were made using an optical line source for SAWs propagating in the [1 1 0] direction in Si, which is taken to be the X-axis in Fig. 1. The interface between the film and the substrate was the (0 0 1) plane of Si, which is normal to the Z-axis in the frame of reference shown in Fig. 1. We assume the line source to be parallel to the Y-direction which is normal to the plane of the paper in Fig. 1. The wave velocities do not depend upon the nature of the source. We model the film as transversely isotropic hexagonal solid with its c-axis parallel to the Z-axis in Fig. 1.

The calculated dispersion curves in the [1 1 0] and [1 0 0] directions of Si are shown in Fig. 2 assuming a perfect interface, that is $\boldsymbol{\beta} = \mathbf{I}$. For these calculations, the following values were used for the material parameters of Si:

$$c_{11}^* = 165.7\,\text{GPa}, \quad c_{12}^* = 63.9\,\text{GPa}, \quad c_{44}^* = 79.6\,\text{GPa}, \quad \rho = 2331\,\text{kg/m}^3$$

Table 1
Density and elastic constants of TiN film that give good fit with the measured dispersion curve in the [1 1 0] direction. Reference set taken from [3] (ρ—density in (kg/m^3), c_{ij}—elastic constants in (Gpa))

	ρ	c_{11}	c_{13}	c_{33}	c_{44}	$Q \times 10^6$
Reference set	5408	455	148	446	159	8.1
Set 1 (iso)	5408	455	150	455	153	6.1
Set 2	5524	478	125	240	275	7.9
Set 3	5505	479	125	230	159	7.1
Set 4	5408	452	120	306	142	7.3
Set 5	5403	455	149	437	175	7.5
Set 6	5408	455	144	416	159	6.7
Set 7	5361	448	144	443	125	7.3

The asterisks over c denote that these values are with respect to the crystallographic axes of silicon. The material parameters of the film chosen for these calculations are taken from Ref. [3]. These parameters are given in row 1 (reference set) of Table 1 in the next section where we will discuss their determination in detail.

The calculated dispersion curves are shown in Fig. 2 for frequencies from 0 to about 20 GHz in order to illustrate the nature of the SAW dispersion in the low as well as high frequency limit. In practice, the measurements are usually limited to the range 15–500 MHz. As seen in Fig. 2, the SAW velocity at zero frequency is equal to 5.08 km/s in the [1 1 0] direction and 4.92 km/s in the [1 0 0] direction. These are the Rayleigh wave velocities in the Si substrate in the two directions and are independent of the film. This is physically expected because the zero frequency wave has infinite wave length which cannot be sensitive to properties of a film of finite thickness. At the other extreme of infinite frequencies, the SAW velocity reduces to 4.93 km/s which is the Rayleigh velocity in the film and does not depend upon the material parameters of the substrate. In this limit the wave is confined to the film and does not see the substrate. As we see from Fig. 2, the Rayleigh velocity of the film is independent of the direction of wave propagation. This is a consequence of the assumed transverse isotropy of the film.

In order to see the effect of the imperfect bonding, we calculate the dispersion curves for the same material system for two values of the debonding parameter: $\beta_1 = 1.5$ and $\beta_1 = 0.5$ while $\beta_3 = 1$. The boundary condition given by Eq. (2.5) for the continuity of the traction is still valid. The values of β_i are chosen just for the purpose of illustration and have no particular physical justification. An experimental analysis of the effect of defective interfacial bonding on SAW propagation is not available. The solution for the virtual forces corresponding to these boundary conditions is given in Appendix A. The calculated dispersion curves are shown in Fig. 3 for the [1 1 0] direction.

For the purpose of comparison, the SAW dispersion for the perfectly bonded film TiN film of thickness 306 nm is also shown in Fig. 3. As expected, the curve for $\beta_1 = 1$ (perfect bonding) in Fig. 3 lies between those for $\beta_1 = 1.5$ and $\beta_1 = 0.5$. We also observe from the figure that the SAW velocity in the zero frequency and the high frequency limits does not depend upon the values of the debonding parameter β. This is physically expected for reasons described previously.

Now we consider the effect of an intermediate layer between the film and the substrate on the SAW dispersion. In general, an intermediate layer almost always exists between the film and the substrate. For example, Si usually has a layer of oxide on the surface. Moreover, there are usually residual stresses at the interfaces. The residual stresses do not change the elastic constants in the linear approximation. In the nonlinear case, the higher order elastic constants can be approximately included by using effective values of the second order elastic constants. Thus it is possible to model the residual stresses at the interface by assuming an intermediate layer of different elastic constants. The calculation of SAW dispersion in case of an intermediate layer follows essentially on the same lines as described above.

The calculated SAW dispersion curve for a TiN film on Si with an intermediate layer of fused silica is shown in Fig. 4. The fused silica is assumed to be isotropic with the following material parameters: $c_{11} = 78.5$ GPa, $c_{12} = 16.1$ GPa, and $\rho = 2204$ kg/m^3. The dispersion curve in Fig. 3 is shown only up to about 500 MHz which is the range of interest from the point of view of measurements. We assume the same geometry as in Fig. 1.

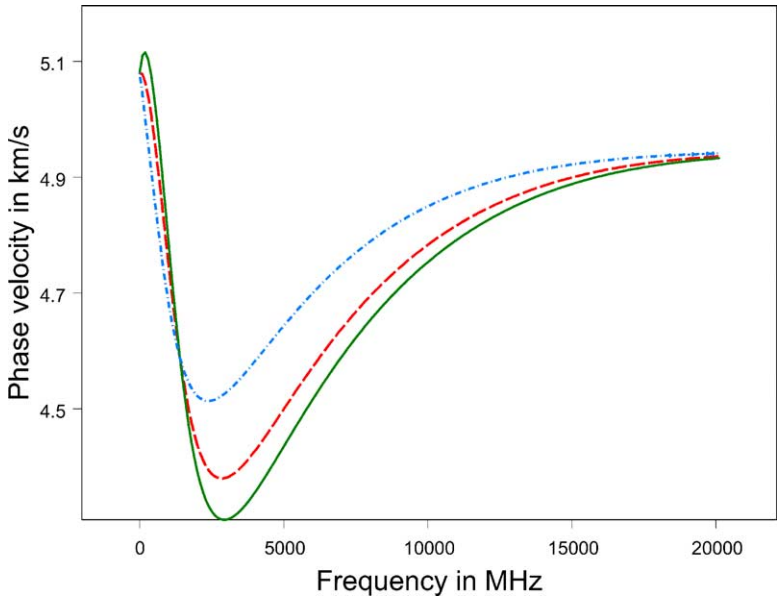

Fig. 3. Dispersion curves in the [1 1 0] direction for a imperfectly bonded 306 nm TiN film on Si calculated by using same parameters as in Fig. 2. Solid line: $\beta_1 = 1.5$; dotted line: $\beta_1 = 0.5$; dashed line: $\beta_1 = 1$ which corresponds to perfect bonding.

The thickness of the film and that of the intermediate layer are assumed to be 206 and 100 nm, respectively. For comparison, the SAW dispersion for TiN film of thickness 306 nm is also shown in the same figure. Again we note that the SAW velocity at zero frequency does not depend upon the properties of the film or the intermediate layer.

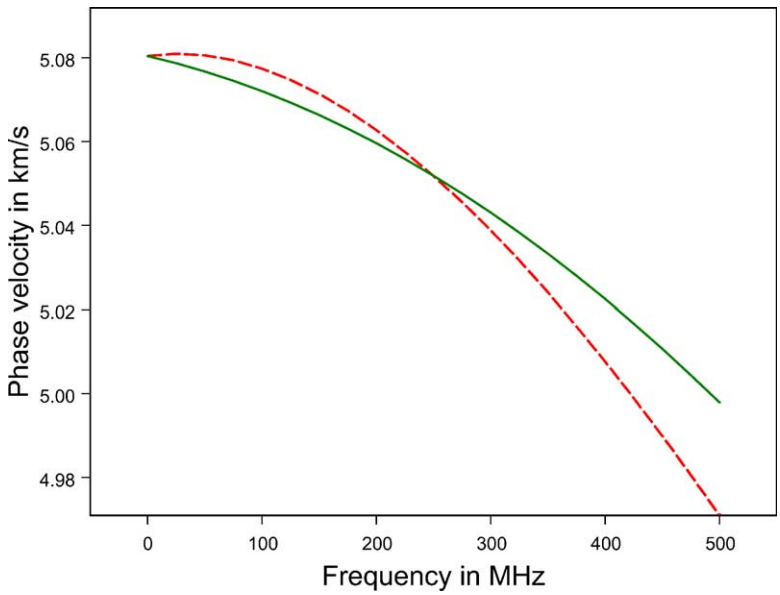

Fig. 4. Dispersion curves in the [1 1 0] direction for a TiN film on Si with an intermediate layer of fused silica. Thickness of the film is 206 nm and that of the silica layer is 100 nm. Solid line: no intermediate layer; dashed line: including layer of silica.

We can draw some general inferences from the dispersion curves in Figs. 2–4 for the purpose of extracting information about the film. At very low frequencies, the SAW velocity is not sensitive to the material parameters of the film, the quality of the bond, or the presence of an intermediate layer. In the limit of infinite frequency, the SAW velocity becomes equal to the Rayleigh velocity in the film independent of its thickness. The Rayleigh velocity is determined by a single combination of elastic constants and density. The Rayleigh velocity is independent of frequency (no dispersion) and can yield only a single parameter. Thus, the SAW dispersion cannot yield all the parameters of the film in the limit of very high frequencies. When the frequencies are such that the wavelength of SAW is comparable to the thickness of the film, then the SAW dispersion will be most sensitive to the parameters of the film. The figures show maximum structure around 3–5 GHz where the SAW measurements should be most sensitive to the presence of the film. Currently, most measurements of SAW dispersion are limited to frequencies > 15 MHz and < 1 GHz.

We make an interesting observation from Figs. 3 and 4. Though the SAW velocity at zero frequency depends only upon the parameters of the substrate, the slope of the dispersion curve at zero frequency is quite sensitive to the parameters of the film. In the absence of the film, SAW propagation will be dispersionless and the slope of the curve would be zero. This would suggest that a direct measurement of the slope of the dispersion curves rather than of the actual velocity as a function of frequency can yield useful information about the film and its bonding with the interface even at low frequencies. Direct measurements of the slopes of the dispersion curves have not been reported in the literature. This also suggests that a measurement of group velocity rather than the phase velocity may give more information about the film since it involves the derivative of the frequency. For Rayleigh waves, the phase and group velocities are equal.

3. Determination of elastic constants of the film from measured SAW dispersion

Experimentally, one measures the SAW dispersion—the phase velocity of the surface waves as a function of frequency. These measurements can, in principle, be inverted to estimate material parameters such as the elastic constants, density, the thickness of the film, and the quality of the interfacial bond. The usual procedure (see, for example, [19]) of obtaining the elastic constants from the measured dispersion is to use a least-squares fit between the observed dispersion curves and theoretical curves obtained by Adler's method [17]. It involves a large number of forward calculations. One difficulty in this procedure lies in the identification of the right branch of the theoretical dispersion curves. If the determinant D_V is $3n \times 3n$, Eq. (2.13) will have $3n$ branches of solutions. Only one of them will correspond to the experimental curve. The difficulty is further aggravated by the crossing over of the branches in the $\boldsymbol{\xi}$-space in some cases.

An efficient method of inversion has been developed at NIST [3]. In this method of inversion, we use the measured values of $\boldsymbol{\xi}$ (inverse velocity) for specific values of ω directly in Eq. (2.13), and solve the resulting nonlinear equation for the material parameters. This method is computationally faster and more efficient and avoids the problem of identification of a specific branch of the solution. In the case of a line source used in the experiment, $\boldsymbol{\xi}$ is a scalar and equal to q_1. Each pair of values of (ω, q_1) gives one equation. We have to use at least as many equations as the number of parameters to be determined. In practice, we choose about double the number of equations, and obtain the parameters by an optimization or minimization procedure.

We consider the same example of TiN film on Si. The values of the elastic constants and the density of the film as calculated in Ref. [3] by using the measured SAW dispersion curve are given in row 1 of Table 1. We will refer to this set of parameters as the reference set. These values were obtained by assuming the film to have transverse isotropy and a perfect interfacial bond for which $\boldsymbol{\beta} = \mathbf{I}$. The measured [1] dispersion curve in the [1 1 0] direction is shown by the triangles in Fig. 5 along with the theoretical curve [3]. The theoretical curve is the lower frequency end of the curve shown in Fig. 2. It is given here again in order to show the agreement with the measured values that are available until about 450 MHz. The fit between the theoretical and the experimental values as shown in Fig. 5 is very good, the difference being less than 0.1%. However, since the measurements are made on only one plane, only four elastic constants—c_{11}, c_{13}, c_{33}, and c_{55}—could be determined.

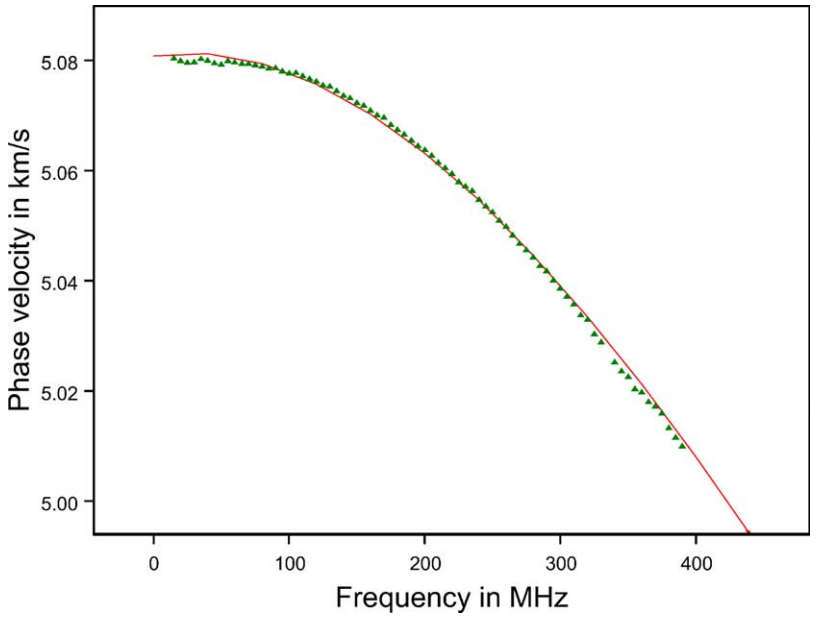

Fig. 5. Theoretical and experimental dispersion curves in the [1 1 0] direction for the same system as in Fig. 2. Solid line: theory; triangles: measured values [1].

The fact that such a good fit is obtained between the theory and the experiment should not be surprising as such, because of a large number (5) of adjustable parameters in the theory. Perhaps the most important question in any inversion algorithm is the uniqueness and the uncertainty in the values of parameters because inversion is essentially an ill posed problem. A set of parameters obtained by inversion can be guaranteed to be unique only if all the measurements can be made at all points which is obviously not possible. Mathematically the lack of uniqueness can be attributed to the solution of the set of nonlinear equations that admit a large number of solutions. One has to find a solution "near" a set of values. In practice, the initial set of values is chosen on physical considerations, but that is not always possible.

We now examine whether the above inversion algorithm gives unique values of the material parameters. We define a quality of fit parameter as follows:

$$Q = \frac{1}{N}\sum_{k}[D_{\mathrm{V}}(q_{1k},\ \omega_k,\ c_{ij},\ \rho,\ a)]^2 \tag{3.1}$$

where q_{1k} and ω_k for k 1, 2,..., N are N points on the observed dispersion curve. If D_{V} is complex, Q could be defined in terms of the magnitude of D_{V}. In general, Q is positive. In the ideal case $Q = 0$. For brevity, we have not shown the function dependence of Q on various parameters. The Q value for the set of parameters for TiN [3] quoted in column 1 of Table 1 is less than 10^{-6} which is quite good. It was mentioned in Ref. [3] but not discussed in any detail that several alternative sets of parameters are possible that give almost as good a fit between the experimental and theoretical SAW dispersion curves in the [1 1 0] direction. We used our inversion algorithm to determine other sets of parameters of the film from the same measured values of SAW dispersion in the [1 1 0] direction.

In general, a set of nonlinear equations, which we have to solve for determining the material parameters, admits many solutions. The nonlinear equations are usually solved by a minimization or an optimization procedure. Such procedures always introduce a nonzero numerical noise. In choosing a set of parameters, we have to define the criteria for the goodness of the solution. In practice, we cannot demand that Q must be 0 for a set of parameters to be acceptable. Moreover, in real cases, there is also a nonzero experimental error. Hence we have to consider

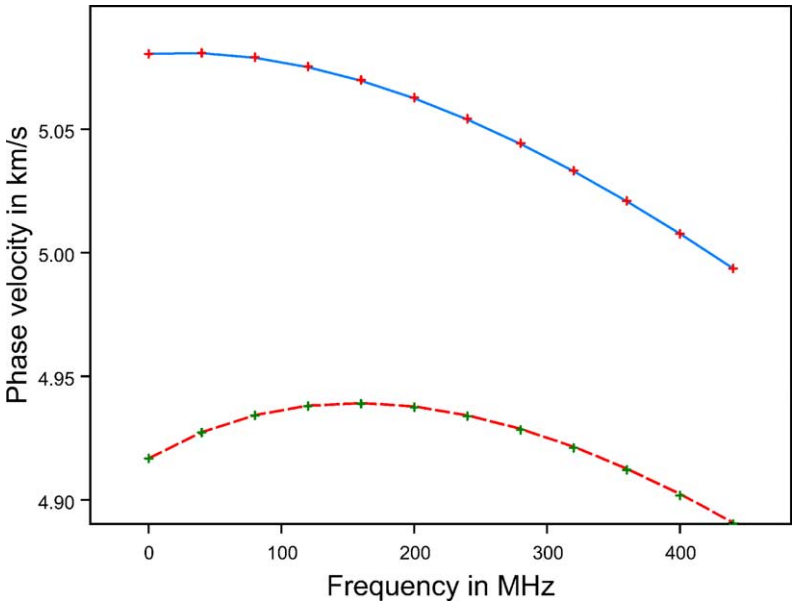

Fig. 6. Dispersion curves in the [1 1 0] and [1 0 0] directions for the same system as in Fig. 2 calculated by using material parameters of sets 2–8 in Table 1. All the sets give approximately the same dispersion curve in both the directions. The values obtained from the reference set are shown as discrete points. Solid line: [1 1 0]; dashed line: [1 0 0].

the uniqueness of the parameters within the margins set by the numerical noise and the experimental error. We arbitrarily choose $Q < 10^{-5}$ for accepting a set of parameters. We also consider the dispersion in the frequency range 10–500 MHz which is the usual range of measurements.

In our inversion algorithm, we used interpolated experimental values in order to reduce the numerical noise caused by the scatter in the experimental values which was very small. We found a large number (at least 20) of sets of parameters that 'fit' the calculated values with the experimental values. Some of these can be ruled out on physical considerations since we know that the film is TiN. We can use constraints such as, for example, that the density should be around 5400 kg/m^3 which is approximately the value for a perfect fcc TiN crystal, c_{11} should be around 400–600 GPa, c_{55} and c_{13} should not be larger than c_{11}, etc. In fact the results are very sensitive to the density, which in real cases can vary because of the varying nitrogen content in TiN. Even constraining the density to a value near 5400 kh/m^3, we found at least 10 sets of parameters which give approximately the same dispersion in the [1 1 0] direction.

Some of the sets of parameters are given in Table 1 in rows 2–8. The calculated dispersion curve obtained from these sets is shown as the dotted line in Fig. 6. The difference between the dispersion curves obtained from different sets is too small to be shown in the figure. The calculated values obtained from the reference set are shown as discrete points in the same figure. We see that the all the sets give about give the same dispersion curve in the [1 1 0] direction which also agrees with the reference set. It should be emphasized that it is not the inadequacy of the inversion algorithm that a unique set is not found. On the other hand it shows the power of the inversion algorithm that it has discovered a large number of sets which all give about the same dispersion curves.

Note that the set given in row 2 of Table 1 is isotropic, that is the elastic constants obey the following isotropy conditions:

$$c_{33} = c_{11} \text{ and } c_{11} - c_{12} = 2c_{44} \tag{3.2}$$

Table 1 also gives the Q value for each set as calculated by using experimental values of the dispersion in Eq. (3.1). Note that all these sets give a good fit, that is, $Q < 10^{-5}$. The difference between the Q values is not large enough to distinguish between the sets. It is not logical to choose the set with the smallest Q value as the best set because of the uncertainties introduced by numerical noise in the calculations as well as experimental measurements in real cases. Hence all sets in Table 1 seem to be equally acceptable.

It would appear that the uniqueness can be improved by taking more independent observations in other directions. Since Si substrate is anisotropic, observations in other directions should provide independent data even if the film is isotropic. We therefore consider SAW propagation in the [1 0 0] direction. We have already assumed that the film is transversely isotropic with its hexagonal c-axis parallel to the Z-axis, so $c_{44} = c_{55}$. If the film was not transversely isotropic, then we would need another elastic constant to calculate the dispersion in the [1 0 0] direction. The SAW dispersion in the [1 0 0] direction calculated from the isotropic set is shown as the dashed curve in Fig. 6. All the sets given in rows 2–8 give about the same dispersion curve. Again, the difference between the values calculated from different sets is too small to be shown in the figure.

The values obtained from the reference set in row1 of Table 1 are shown as discrete points on the curve in the same figure. Note that the values calculated from the reference set agree very well with the values obtained from other sets in the [1 0 0] direction also. Hence we infer that if the reference set correctly predicts the measurements in the [1 0 0] direction, so would all the other sets in Table 1. Thus measurements in the [1 0 0] direction would not be able to distinguish between the sets given in Table 1. Note that the SAW velocities in the [1 1 0] and the [1 0 0] directions at zero frequency, which correspond to the Rayleigh velocities in the two directions in Si, as well the starting slope and curvature of the two curves in Fig. 6 are very different. This difference would suggest that the two curves are independent and should contain independent information. It is a consequence of the transverse isotropy of the film that measurements in different directions do not yield new information. However, it is surprising since the substrate is anisotropic. If transverse isotropy is not assumed, more elastic constants will be needed.

The main reason for lack of uniqueness is that there are too many unknown parameters compared to the amount of information contained in the measured values of the SAW dispersion. If the experimental uncertainties and numerical noise is close to zero, it may be possible in principle to find the global minimum of Q that will correspond to the real set of parameters. It would not help very much if we include very high frequencies. As mentioned earlier, in the limit of infinite frequency, the SAW velocity becomes equal to the Rayleigh velocity in the film independent of its thickness. The Rayleigh velocity is determined by a single combination of elastic constants and density. The Rayleigh velocity is independent of frequency (no dispersion) and can yield only a single parameter. Thus, the SAW dispersion cannot yield all the parameters of the film in this limit. As remarked earlier, the most sensitive region of the frequency in this case is about 3–5 GHz when the wavelength of SAW is comparable to the thickness of the film.

If we constrain the elastic constants to obey Eq. (3.2), and allow the density to vary, we still get different sets of parameters. However, if we fix the density along with the isotropy condition, then we do obtain a unique set of isotropic elastic constants. If we constrain the density to vary in a small range, then may be even three parameters—two elastic constants and the density can be determined within the range of numerical noise.

In the anisotropic case also two parameters can be uniquely determined if we fix the values of other parameters. The calculated values are not very sensitive to choice of c_{44} so the estimated values of c_{44} are least reliable. If we fix the density, c_{44}, and c_{33}, then we obtain unique values of c_{11} and c_{13}. In general if we vary only two parameters then we get a unique set but the results are more stable if we fix c_{44}. So it appears that the information content in the SAW dispersion curves is just about enough to determine two parameters or, at the most three parameters if the density is constrained to vary in a small range.

We also used the inversion algorithm to determine the values of the debonding parameter and the parameters of the intermediate layer. The above discussion also applies to these cases. If all other parameters are fixed, then two parameters, for example, the debonding parameter or two elastic constants of the intermediate layer can be determined from the SAW dispersion curves.

The main conclusion is that, for isotropic as well as anisotropic films, two material parameters can be most efficiently determined by SAW measurements by using the known values of other parameters. The calculations are

Table 2
Magnitude of the estimated fractional error in each parameter of the TiN film given in Table 1 due to inadequate fitting as calculated from Eq. (3.4)

	$(\Delta\rho/\rho)\times 10^{-3}$	$(\Delta c_{11}/c_{11})\times 10^{-3}$	$\Delta c_{13}/c_{13}$	$\Delta c_{33}/c_{33}$	$\Delta c_{44}/c_{44}$
Reference set	2.9	4.3	0.02	0.05	0.6
Set 1 (iso)	4.9	8.2	0.05	0.10	0.74
Set 2	4.3	6.9	0.03	0.08	1.2
Set 3	5.7	10	0.05	0.12	0.79
Set 4	5.2	9.1	0.06	0.14	0.69
Set 5	4.9	8.4	0.05	0.11	0.84
Set 6	5.3	9.2	0.05	0.12	0.79
Set 7	5.1	8.8	0.05	0.12	0.61

very sensitive to the density of the film and least sensitive to c_{44}. In general, as remarked in [3], the variation of c_{11} amongst different sets is relatively small. It seems that the best use of the above procedure is for determining the value of c_{11} and the density of films. These conclusions are of course based upon the analysis of a single sample, that is a TiN film on Si.

We now discuss the errors in the values of parameters determined by using the inversion algorithm. There are two main sources or errors: inexact solution of Eq. (2.13) which makes Q nonzero, (ii) errors in the measured values of the input parameters to Eq. (2.13) such as the thickness of the film, elastic constants of the substrate, etc. We use the Newton's formula to estimate the error due to inexact solution of Eq. (2.13). Let w_0 be the exact value of some parameter which is estimated to be w by using the above algorithm. By expanding Q in a Taylor series at w, we obtain from Eq. (3.1)

$$Q(w_0) = Q(w) + \left[\frac{\partial Q}{\partial w}\right](w_0 - w) \tag{3.3}$$

where the derivative is evaluated at w. If w_0 is the exact solution, the LHS of Eq. (3.3) is 0. This gives the following first order estimate of the error in w:

$$\Delta w = (w_0 - w) = -\frac{Q(w)}{\partial Q/\partial w} \tag{3.4}$$

The calculated fractional error $\Delta w/w$ in each parameter of each set of the film is given in Table 2. The set numbers in this table refer to the same set numbers as in Table 1. In principle, Eq. (3.4) provides an additional and independent criterion for choosing between alternative sets since it requires Q to be small and its derivative to be large. This criterion would prefer a sharp minimum (large derivative) over a shallow minimum (small derivative). However, it is more a mathematical rather than physical criterion. There is no obvious reason why the actual values of the parameters should be at a sharp minimum.

Similarly, we can obtain the error in the estimated value of a parameter caused by an error in an input parameter. If w is the estimated parameter and p is an input parameter, we obtain by taking the total derivative of D_V from Eq. (2.13)

$$\frac{\mathrm{d}w}{\mathrm{d}p} = -\frac{\partial V/\partial p}{\partial V/\partial w} \tag{3.5}$$

The fractional error in the estimated value of the parameter w is given by:

$$\frac{\Delta w}{w} = \left(\frac{p}{w}\right)\left(\frac{\mathrm{d}w}{\mathrm{d}p}\right)\left(\frac{\Delta p}{p}\right) \tag{3.6}$$

where $(\Delta p/p)$ is the fractional error in the input parameter p. Eq. (3.6) gives the error in w as a function of the frequency. To estimate the overall error, we use Q in place of D_V in Eq. (3.5). An important source of error in the

Table 3
Magnitude of the estimated fractional error in each parameter of the TiN film given in Table 1 due to fractional error 0.1 in the input value of film thickness as calculated from Eq. (3.6)

	$(\Delta\rho/\rho) \times 10^{-2}$	$(\Delta c_{11}/c_{11}) \times 10^{-2}$	$\Delta c_{13}/c_{13}$	$\Delta c_{33}/c_{33}$	$\Delta c_{44}/c_{44}$
Reference set	2.7	4.0	0.21	0.46	5.5
Set 1 (iso)	3.2	5.3	0.29	0.67	4.8
Set 2	3.0	4.8	0.22	0.52	8.4
Set 3	3.4	6.1	0.28	0.72	4.7
Set 4	3.3	5.8	0.35	0.87	4.4
Set 5	3.2	5.4	0.29	0.68	5.5
Set 6	3.3	5.7	0.32	0.75	4.9
Set 7	3.3	5.7	0.33	0.78	4.0

above determination of material parameters of the film is the thickness of the film. For the purpose of illustration we consider the same model system TiN/Si with perfect interfacial bond. We assume $(\Delta p/p) = 0.1$. The overall errors calculated by using Q instead of D_V in Eq. (3.6) for all the parameters are given in Table 3.

We note from that the fractional error in c_{44} is very large for all the sets and small for c_{11} and the density. This is consistent with the observation made earlier in this section that the solution obtained by the inversion algorithm is sensitive to c_{11} and the density and not sensitive to c_{44}.

4. Conclusions

1. A Green's-function based method developed at NIST, has been described for calculating the SAW dispersion curves in anisotropic material systems such as single as well as multiple thin films on anisotropic substrates. The method is applicable to films with a defective interfacial bond which is simulated by introducing discontinuities in the displacement field at the interface.
2. The formulation is based upon the delta-function representation of the elastodynamic Green's function and provide a computationally efficient inversion algorithm for determining the material parameters of the film from the measured SAW dispersion curves. The parameters which can be, in principle, determined from the SAW dispersion curves include elastic constants, density, bonding defect, and thickness of the film.
3. In the zero frequency limit the SAW velocity in the film is equal to the Rayleigh velocity in the substrate without the film and in the high frequency limit it is equal to the Rayleigh velocity in the film without the substrate. The SAW dispersion curves are therefore not sensitive to the film at low frequencies. In the high frequency limit it depends only upon a single combination of all the parameters of the film that gives the Rayleigh velocity in the material of the film. The most sensitive region of frequencies for determining the material parameters of the film is when the wavelength of the SAW is comparable to the thickness of the film. However, the slope of the SAW dispersion curve is sensitive to the parameters of the film even at low frequencies. A direct measurement of the slope should therefore be useful for interrogating the properties of the film.
4. The uniqueness (or lack of it) of the parameters as determined by using the inversion algorithm is discussed in detail by taking the example of a 306 nm TiN film on Si. It is found that the SAW dispersion curves can give unique values of two parameters which can be the elastic constants and/or the density. If the film is characterized by more than two parameters such as in the general anisotropic case, the inversion process does not yield a unique set of all the parameters even if measurements are made in several directions. SAW dispersion curves can be useful to determine any two parameters including the density provided reliable values of other parameters are available.
5. In the example considered in this paper, the estimated values of c_{11} and the density are found to be most reliable. The values of c_{44} are found to be most unreliable.

Acknowledgements

I thank Dr. C.M. Flannery and Dr. D.C. Hurley for helpful suggestions and discussions.

References

[1] D.C. Hurley, V.K. Tewary, A.J. Richards, Surface acoustic wave methods to determine the anisotropic elastic properties of thin films, Meas. Sci. Tech. 12 (2001) 1486–1494.
[2] D.C. Hurley, V.K. Tewary, A.J. Richards, Thin-film elastic property measurements with laser-ultrasonic SAW spectrometry, Thin Sol. Films 398/399 (2001) 326–330.
[3] V.K. Tewary, Theory of elastic wave propagation in anisotropic film on anisotropic substrate: TiN film on single crystal Si, J. Acoust. Soc. Amer. 112 (2002) 925–935.
[4] V.K. Tewary, Computationally efficient representation for elastodynamic and elastostatic Green's functions for anisotropic solids, Phys. Rev. B 51 (1995) 15695–15702.
[5] A.G. Every, Measurement of the near-surface elastic properties of solids and thin supported films, Meas. Sci. Tech. 13 (2002) R21–R39.
[6] A. Lomonosov, A.P. Mayer, P. Hess, Laser controlled surface acoustic waves, Handbook of Elastic Properties of Solids, Liquids, and Gases, vol. 1, Academic Press, NY, 2001.
[7] A. Mourad, C. Desmet, W. Lauriks, H. Coufal, J. Thoen, The Green's function for surface acoustic waves: Comparison between theory and experiment, J. Acoust. Soc. Amer. 100 (1996) 1538–1541.
[8] C.Y. Wang, J.D. Achenbach, A new method to obtain 3-D Green's functions for anisotropic solids, Wave Motion 18 (1993) 273–289.
[9] A.G. Every, K.Y. Kim, A.A. Maznev, The elastodynamic response of a semi-infinite anisotropic solid to sudden surface loading, J. Acoust. Soc. Amer. 102 (1997) 1346–1355.
[10] T.C.T. Ting, Anisotropic Elasticity: Theory and Applications, Oxford University Press, Oxford, 1996.
[11] V.K. Kinra, V. Dalal, A new technique for ultrasonic-nondestructive evaluation of thin specimens, Exp. Mech. 28 (1988) 288–297.
[12] D.E. Chimenti, Guided waves in plates and their use in materials characterization, Appl. Mech. Rev. 50 (1997) 247–284.
[13] D.M. Barnett, J. Lothe, Free surface (Rayleigh) waves in anisotropic elastic half-spaces: the surface impedance methods, Proc. R. Soc. London A 402 (1985) 135–152.
[14] B.A. Auld, Acoustic Fields and Waves in Solids, vol. I, Robert E. Krieger Publishing Company, Malabar, FL, 1990.
[15] A.H. Nayfeh, Wave Propagation in Layered Anisotropic Media with Applications to Composites, Elsevier, Amsterdam, 1995.
[16] Y. Li, R.B. Thomson, Influence of anisotropy on the dispersion characteristics of guided plate modes, J. Acoust. Soc. Amer. 87 (1990) 1911–1931.
[17] G.W. Farnell, E.L. Adler, Elastic wave propagation in thin layers, in: W.P. Mason, R.N. Thurston (Eds.), Phys. Acoust., vol. 9, Academic Press, NY, 1972, pp. 35–127.
[18] C.M. Flannery, E. Chilla, S. Semenov, H.-J. Fröhlich, Elastic properties of GaAs obtained by inversion of laser-generated surface acoustic wave measurements, in: S.C. Schneider, M. Levy, B.R. McAvoy (Eds.), Proceedings of IEEE Ultrasonics Symposium,1999, pp. 501–504.
[19] D. Schneider, T. Schwarz, B. Schultrich, Determination of elastic modulus and thickness of surface layers by ultrasonic surface waves, Thin Sol. Films 219 (1992) 92–102.
[20] J.D. Achenbach, Wave Propagation in Elastic Solids, Elsevier, Amsterdam, 1973.
[21] J.R. Willis, Self-similar problems in elastodynamics, Phil. Trans. R. Soc. London A 274 (1973) 435–491.
[22] S.C. Ren, N.N. Hsu, D.G. Eitzen, Transient Green's tensor for a layered slid half-space with different interface conditions, J. Res. NIST 107 (2002) 445–473.